Mobility of Circular and Elliptical Si Nanowire Transistors Using a Multi-Subband 1D Formalism

C. Medina-Bailon, T. Sadi, M. Nedjalkov, H. Carrillo-Nuñez, J. Lee, O. Badami, V. Georgiev,
S. Selberherr, *Fellow, IEEE,* and A. Asenov, *Fellow, IEEE*.

Abstract—We have studied the impact of the cross-sectional shape on the electron mobility of n-type silicon nanowire transistors (NWTs). We have considered circular and elliptical cross-section NWTs including the most relevant multisubband scattering processes involving phonon, surface roughness, and impurity scattering. For this purpose, we use a flexible simulation framework, coupling 3D Poisson and 2D Schrödinger solvers with the semi-classical Kubo-Greenwood formalism. Moreover, we consider cross-section dependent effective masses calculated from tight binding simulations. Our results show significant mobility improvement in the elliptic NWTs in comparison to the circular one for both [100] and [110] transport directions, especially when surface roughness scattering is included.

Index Terms—One-Dimensional Multi-Subband Scattering Models; Transport Effective Mass; Kubo-Greenwood Formalism; Quantum Confinement; Nanowire Field-Effect Transistors

I. Introduction

In recent years, there has been a huge interest in the study and the modelling of the impact of material and geometrical features of Gate-all-around (GAA) nanowire transistors (NWTs) [1]–[5]. They are being considered as potential candidates to extend the CMOS technology beyond the 7 nm node [6] due to the better electrostatic integrity compared to Fully-Depleted Silicon-On-Insulator (FDSOI) [7] transistors and FinFETs [8]. To underpin these technology projections, it is important to study the impact of the NWT cross-sectional shape at the scaling limit on the transistor performance. Quantum confinement effects modify the electron distribution in the subbands, determining the charge available for transport [9], [10], and, consequently, the matrix elements of the coupling with the phonons and the electrostatic potential profile [11].

The aim of this letter is to perform a conclusive study of the impact of the cross-sectional shape on the low-field electron mobility in silicon NWTs. The novelty of this work is in both the type of analysis and results presented, and the model features. In particular, circular and elliptic cross-sectional shapes are compared for technology-relevant material orientations with state-of-the-art diameters, corresponding to

current miniaturization trends (≤ 8 nm), showing the superior performance of the latter shape. For both shapes, we present in a transparent manner the impact of the different scattering mechanisms individually on the low-field electron mobility. For this purpose, we employ a one-dimensional (1D) multisubband approach which combines quantum effects with the semi-classical Boltzmann transport equation (BTE) in the relaxation time approximation for a 1D electron gas. We adopt the Kubo-Greenwood (KG) formalism [12]–[14], while accounting for the realistic band structure of the NWTs by accurately extracting the effective masses from tight-binding band-structure simulations. This strategy delivers reliable mobility values at low-field near-equilibrium conditions and in devices with strong confinement effects [15].

II. Methodology

Fig. 1 illustrates the simulated NWTs and lists the corresponding device parameters. The nanowire width ranges from 3 nm to 8 nm for both the circular and the elliptical cross-sections, considering [100] and [110] transport directions. For the elliptic NWT, the ratio between the major (y direction) and minor (z direction) diameters remains 1.5. Supplemental simulations with the ratio ranging from 1 to 2 (not shown) suggest that 1.5 presents the optimum ratio. We have taken into account this diameter range due to the well-established transition from fully-quantum behavior at 3 nm with strong confinement impact [16], and large effective mass deviation [17]; to near bulk-like electronic behavior at 8 nm [18].
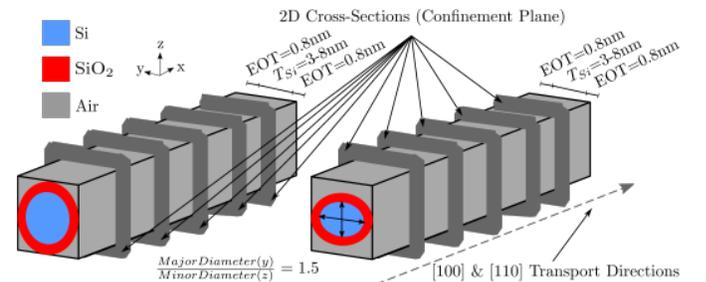
Fig. 1: Circular and elliptic NWT structures analyzed in this work with widths ranging from 3 nm to 8 nm. The coupled 3D Poisson and 2D Schrödinger equations are solved for each cross-section (confinement plane) and then the scattering rates are calculated for each subband.

The rest of the technological parameters remains identical: the gate oxide has an equivalent oxide thickness (EOT) of 0.8 nm, the metal gate work function is set to 4.35eV, and room temperature (300K) is assumed. In order to accurately reproduce the quantum behavior for diameters smaller than

8 nm, we have extracted [19] the transport and the confinement effective masses from an empirical sp^{3}d^{5}s* tight-binding simulations with the Boykin's parameter set [20] implemented in QuantumATK from Synopsys [21]. Furthermore, as the surface roughness scattering mechanism dominates the mobility for very high sheet concentrations, all the mobility results are reported at the medium carrier concentration 2.8×10^{12} cm^{-2} [16], [17], [22]. The gate bias is adjusted to obtain the sheet concentration (cm^{-2}) being computed as the line density (cm^{-1}) divided by the total perimeter.

The mobility calculation approach here considered is based on long-channel simulations. First, multiple cross-sections of the device are simulated (Fig. 1) to pre-calculate the potential distribution and the corresponding eigenfunctions considering a low electric field (1 kV/cm) in the transport direction. In this particular work, we have run all the simulations using the coupled 3D Poisson and 2D Schrödinger solver integrated in the TCAD simulator GARAND from Synopsys [23].

Second, the different scattering rates, which expressions have been directly developed from the Fermi Golden rule accounting for the multi-subband quantization in the confinement plane, are calculated. The following scattering mechanisms have been used in this paper (more details of these mechanisms as well as their equations can be found in [16], [17], [22]): (i) acoustic phonon (Ac Ph) scattering; (ii) optical phonon (Op Ph) scattering, with fixed parameters for the different branches; (iii) surface roughness (SR) scattering, with root mean square (Δ_{RMS}) and correlation lengths 0.48 nm and 1.3 nm, respectively; and (iv) ionized impurity (II) scattering, with a constant effective ionized impurity concentration N_I=10^{18}cm^{-3}.

Third, the mobilities with different scattering mechanisms are independently calculated by adopting the KG formalism. Finally, the Matthiessen rule is used to determine the combined effect of the scattering mechanisms [24]. Coupling this framework significantly reduces the computational time in comparison to the full scale Monte Carlo or Non-Equilibrium Green's Function (NEGF) simulations including scattering.

III. RESULTS AND DISCUSSION

In the KG formalism, the mobility decreases with the increasing scattering rate, as calculated following the momentum relaxation time approach. The subband levels and the overlap factors (OFs) play the most important role in determining the different rates, as discussed in Ref. [22]. Figure 2(a) illustrates the difference between the first and the second energy subband levels (E_{12}) for different valleys, while Fig. 2(b) shows the difference between the smallest and the largest first subband energies among the delta valleys (E_Δ), for [100] and [110] transport directions, all for the circular and elliptic NWTs, and as a function of the cross-sectional area. The total number of subbands considered in each valley (X1, X3 and X5) for all simulations is 20. From Fig. 2(a), E_{12} is highest for the circular NWTs, increasing as the area (diameter) is decreased, leading to lower intravalley multisubband transitions and hence a possible boost in the mobility at lower diameters. However, such a boost is countered by a significantly lower E_Δ for the circular NWT, as highlighted in Fig. 2(b), which degrades

mobility as compared to the elliptic NWTs. Indeed, as the effect of E_Δ is more dominant [1], a much lower value indicates more electron transitions to upper valleys with higher transport masses, adversely affecting the low-field mobility.
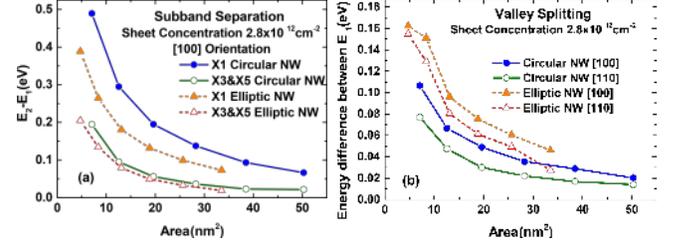
Fig. 2: (a) Difference between the first and the second energy subband levels for the circular and elliptic NWTs and [100] transport direction, as a function of the area. (b) Difference between the smallest and the largest first subband energies among the delta valleys as a function of the area for the circular and elliptic NWTs as well as for [100] and [110] transport directions.

The OF is an integral, over the cross-sectional area along the confinement directions normal to the 1D transport direction, of the wavefunction in the initial subband multiplied by the wavefunction in the final valley. Fig. 3 shows example OFs as a function of the area for both NWT shapes, which are calculated for the fundamental subband (first subband of valley X3) and intra-valley transitions. In general, the increase in the OF at smaller diameters is a direct result of modifying the population and wavefunction features of different subbands in smaller cross-sections [5], [11]. Subsequently, the scattering rates, which are directly proportional to the OF, generally increase with the area reduction. As the NWT area is the main factor determining the OF, this quantity is almost identical for different NWT shapes at the same area, as depicted in Fig. 3.
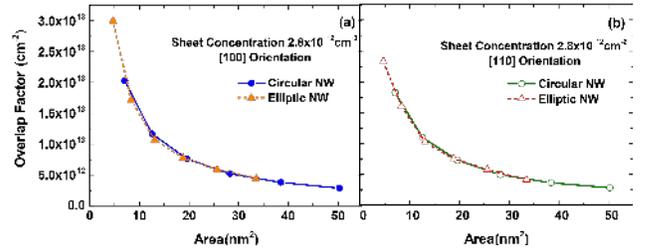
Fig. 3: Overlap factor for the circular and elliptic NWT as a function of the area for (a) [100] and (b) [110] transport directions, being calculated for the fundamental subband (1st subband of valley X3) and intra-valley transitions.

Two different conclusions can be summarized: (i) the electron mobility decreases with the area because it is inversely proportional to the scattering rates; (ii) when we extrapolate this study between shapes, as the area is not a mobility booster (Fig. 3) and due to the higher intervalley separation (Fig. 2(b)), and hence the lower transition rates to high transport mass upper valleys, the elliptical shape enhances the mobility in comparison to the circular one. These trends are clearly demonstrated in Fig. 4 (a)/(c), where the electron mobility as a function of the NWT area is shown for both circular and elliptic NWTs with [100] and [110] transport directions, respectively, considering the impact of the 'Ph' scattering, the combined 'Ph+SR' scatterings, and all simulated scattering mechanisms 'Ph+SR+II'. This mobility trends also holds when plotting the mobility as a function of the average diameter, as shown Fig. 4 (b)/(d), which is calculated as the average

between the major and the minor diameters. Interestingly, the superior transport properties in the elliptical NWT is complemented by superior electrostatic performance reported previously [11]. As expected [25], and for both comparisons as a function of the area and the average diameter, the electron mobility is higher in the [110] (Fig. 4 (c)/(d)) transport direction than in the [100] (Fig. 4 (a)/(b)).
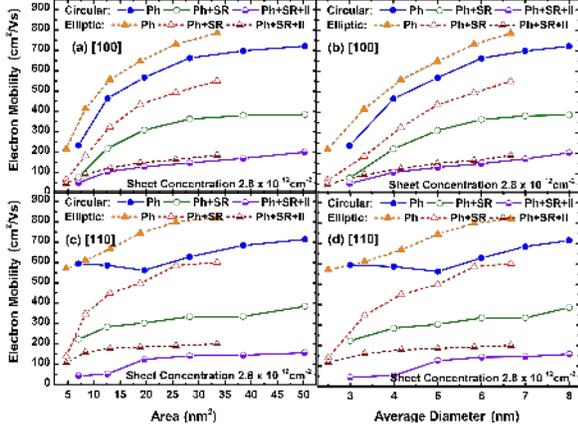
Fig. 4: Electron mobility as a function of the area (a)/(c) and the average diameter (b)/(d), considering the impact of the phonon scattering effect (Ph), the combined phonon and surface roughness (Ph+SR) scattering effects, and all simulated scattering mechanisms (Ph+SR+II). The results are for circular and elliptic NWTs and [100] (a)/(b) and [110] (c)/(d) transport directions.

To illustrate better the electron mobility enhancement in the elliptic NWTs, in comparison to circular transistors, we plot, in Fig. 5, the mobility improvement $\mu_\% = 100 \cdot |\mu_{Elliptic} - \mu_{Circular}|/\mu_{Elliptic}$ in the three scattering limited mobility cases: the 'Ph' scattering case, the combined 'Ph+SR' case, and the combined 'Ph+SR+II' case. Close inspection of Fig. 5(a) considering the [100] transport direction shows that the improvement steeply increases for areas smaller than 12.5 nm^2. For instance, if we compare the Ph limited mobility, the improvement varies from ~30% for the smallest area to ~15% for the widest device considered here. Second, the improvement is more noticeable when we include SR along with the Ph limited mobility, whereas it decreases to the Ph levels when additionally including the less relevant II scattering (Ph+SR+II). Specifically, the maximum improvement occurs when including SR. As this mechanism's rate depends on the electrostatic force normal to the Si-SiO$_2$ interface; the lower SR impact on the elliptic NWTs in comparison to the circular ones highlights the connection between SR scattering, the electric field distribution, and the cross-sectional shape. Then, as we have considered a fixed ionized impurity concentration (independently of the width or shape), this mechanism affects in a similar fashion both NWT shapes. Finally, different result can be found when the [110] transport orientation is considered (Fig. 5 (c)). First, the Ph enhancement is reduced for smaller areas varying from ~2.5% for the narrowest area to ~25% for the widest area. Second, the improvement when SR is included to the Ph electron limited mobility is similar to the [100] direction (improvement of ~10-15% with respect to Ph). Third, the total mobility (Ph+SR+II) is much more affected when II is included for the circular NWT than for the elliptic one (Fig. 4 (c)) for areas lower than 20 nm^2. As it is the

case in Fig. 4, the same trend holds when the difference is represented as a function of the average diameter for both transport directions in Fig. 5 (b)/(d). The high enhancement in [110] when including II scattering is not useful, as the mobility in this case is very low.
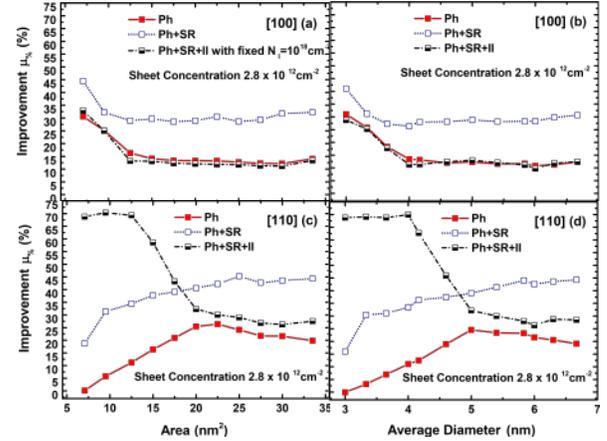
Fig. 5: Improvement (in % points) of the electron mobility for the elliptic and the circular NWTs as a function of the area (a)/(c) and the average diameter (b)/(d), considering the impact of the phonon scattering effect (Ph), the combined phonon and surface roughness (Ph+SR) scattering effects, and all simulated scattering mechanisms (Ph+SR+II). The results are for [100] (a)/(b) and [110] (c)/(d) transport directions.

The presented long-channel mobilities are fully valid for channels whose length is larger than the electron mean-free-path. Short channel devices tend to operate near the ballistic region but scattering continues to be relevant. Clear correlation between mobility and performance is established in many simulation and experimental studies down to the nanoscale [26], [27]. There is a strong link between mobility and the backscattering coefficient that determines the degree of ballisticity. Hence, the long-channel mobilities are still relevant in short channel devices. In extremely short channels with pure ballistic transport, fully quantum transport models based e.g. on the NEGF formalism with scattering mechanisms may be used for more reliable predictions [28], [29].

IV. CONCLUSIONS

We demonstrated the impact of the geometry on the low-field electron mobility of silicon NWTs, by comparing nanowires with circular and elliptic cross-sectional shapes. To do so, we use a quantum corrected semi-classical approach combining: effective masses calibrated from tight-binding simulations, quantum effects based on the rates of the relevant 1D multisubband scattering mechanisms, and the semi-classical Boltzmann transport equation in the relaxation time approximation adopting the Kubo-Greenwood formalism. The most important result show that less pronounced upper intervalley transitions are generally obtained from the elliptic NWT in comparison to the circular one for the same cross-sectional area, leading to a significant mobility improvement. This improvement is more visible when including surface roughness scattering. Finally, despite the mobility increase in both shapes when the [110] transport direction is considered, the improvement introduced by using the elliptic shape is reduced for smaller area.

References

[1] T. Sadi, E. Towie, M. Nedjalkov, C. Riddet, C. Alexander, L. Wang, V. Georgiev, A. Brown, C. Millar, and A. Asenov, "One-dimensional multi-subband Monte Carlo simulation of charge transport in Si nanowire transistors," in *2016 International Conference on Simulation of Semiconductor Processes and Devices (SISPAD)*. IEEE, 2016, pp. 23–26, DOI: 10.1109/SISPAD.2016.7605139.

[2] Y. Li and C.-H. Hwang, "The effect of the geometry aspect ratio on the silicon ellipse-shaped surrounding-gate field-effect transistor and circuit," *Semiconductor Science and Technology*, vol. 24, no. 9, p. 095018, 2009, DOI: 10.1088/0268-1242/24/9/095018.

[3] L. Zhang, L. Li, J. He, and M. Chan, "Modeling short-channel effect of elliptical gate-all-around MOSFET by effective radius," *IEEE Electron Device Letters*, vol. 32, no. 9, pp. 1188–1190, 2011, DOI: 10.1109/LED.2011.2159358.

[4] S. Kumar and S. Jha, "Impact of elliptical cross-section on the propagation delay of multi-channel gate-all-around MOSFET based inverters," *Microelectronics Journal*, vol. 44, no. 9, pp. 844–851, 2013, DOI: 10.1016/j.mejo.2013.06.003.

[5] T. Al-Ameri, V. P. Georgiev, T. Sadi, Y. Wang, F. Adamu-Lema, X. Wang, S. M. Amoroso, E. Towie, A. Brown, and A. Asenov, "Impact of quantum confinement on transport and the electrostatic driven performance of silicon nanowire transistors at the scaling limit," *Solid-State Electronics*, vol. 129, pp. 73–80, 2017, DOI: 10.1016/j.sse.2016.12.015.

[6] B. Yu, H. Wang, C. Yang, P. Asbeck, and Y. Taur, "Scaling of nanowire transistors," *IEEE Transactions on Electron Devices*, vol. 55, no. 11, pp. 2846 – 2858, 2008, DOI: 10.1109/TED.2008.2005163.

[7] Q. Liu, B. DeSalvo, P. Morin, N. Loubet, S. Pilorget, F. Chafik, S. Maitrejean, E. Augendre, D. Chanemougame, S. Guillaumet, H. Kothari, F. Allibert, B. Lherron, B. Lui, Y. Escarabajal, K. Cheng, J. Kuss, M. Wang, R. Jung, S. Teehan, T. Levin, M. Sankarapandian, R. Johnson, J. Kanyandekwe, H. He, R. Venigalla, T. Yamashita, B. Haran, L. Grenouillet, and M. Vinet, "FDSOI CMOS devices featuring dual strained channel and thin BOX extendable to the 10nm node." 2014 IEEE International Electron Devices Meeting (IEDM), 2014, pp. 9.1.1 – 9.1.4., DOI: 10.1109/IEDM.2014.7047014.

[8] W. Yang, Z. Yu, and L. Tian, "Scaling theory for FinFETs based on 3-D effects investigation," *IEEE Transactions on Electron Devices*, vol. 54, no. 5, pp. 1140–1147, 2007, DOI: 10.1109/TED.2007.893808.

[9] G. Chindalore, S. A. Hareland, S. A. Jallepalli, A. F. Tasch, C. M. Maziar, V. K. F. Chia, and S. Smith, "Experimental determination of threshold voltage shifts due to quantum mechanical effects in MOS electron and hole inversion layers," *IEEE Electron Device Letters*, vol. 18, no. 5, pp. 206–208, 2007, DOI: 10.1109/55.568765.

[10] H. Takeda and N. Mori, "Three-dimensional quantum transport simulation of ultra-small FinFETs," *Journal of Computational Electronics*, vol. 4, no. 1–2, pp. 31 – 34, 2005, DOI: 10.1007/s10825-005-7102-0.

[11] Y. Wang, T. Al-Ameri, X. Wang, V. P. Georgiev, E. Towie, S. M. Amoroso, A. R. Brown, B. Cheng, D. Reid, C. Riddet, L. Shifren, S. Sinha, G. Yeric, R. Aitken, X. Liu, J. Kang, and A. Asenov, "Simulation study of the impact of quantum confinement on the electrostatically driven performance of n-type nanowire transistors," *IEEE Transactions on Electron Devices*, vol. 62, no. 10, pp. 3229–3236, 2015, DOI: 10.1109/TED.2015.2470235.

[12] D. Ferry and C. Jacoboni, *Quantum transport in semiconductors*. Berlin, Germany: Springer Science & Business Media, 1992.

[13] S. Jin, T.-W. Tang, and M. V. Fischetti, "Simulation of silicon nanowire transistors using boltzmann transport equation under relaxation time approximation," *IEEE Transactions on Electron Devices*, vol. 55, no. 3, pp. 727–736, 2008, DOI: 10.1109/TED.2007.913560.

[14] D. Esseni, P. Palestri, and L. Selmi, *Nanoscale MOS Transistors: Semiclassical Transport And Applications*. New York, USA: Cambridge University Press, 2011.

[15] I. M. Tienda-Luna, F. G. Ruiz, A. Godoy, B. Biel, and F. Gámiz, "Surface roughness scattering model for arbitrarily oriented silicon nanowires," *Journal of Applied Physics*, vol. 110, no. 8, p. 084514, 2011, DOI: 10.1063/1.3656026.

[16] C. Medina-Bailon, T. Sadi, M. Nedjalkov, J. Lee, S. Berrada, H. Carrillo-Nuñez, V. Georgiev, S. Selberherr, and A. Asenov, "Study of the 1D Scattering Mechanisms' Impact on the Mobility in Si Nanowire Transistors." 2018 Joint International EUROSOI Workshop and International Conference on Ultimate Integration on Silicon (EUROSOI-ULIS), 2018, pp. 1–4, DOI: 10.1109/ULIS.2018.8354723.

[17] ——, "Impact of the Effective Mass on the Mobility in Si Nanowire Transistors." 2018 International Conference on Simulation of Semiconductor Processes and Devices (SISPAD), 2018, pp. 297–300, DOI: 10.1109/SISPAD.2018.8551630.

[18] Z. Stanojević, O. Baumgartner, V. Sverdlov, and H. Kosina, "Electronic band structure modeling in strained Si-nanowires: Two band k·p versus tight binding." International Workshop on Computational Electronis (IWCE), 2010, pp. 1–4, DOI: 10.1109/IWCE.2010.5677927.

[19] O. Badami, C. Medina-Bailon, S. Berrada, H. Carrillo-Nunez, J. Lee, V. Georgiev, and A. Asenov, "Comprehensive Study of Cross-Section Dependent Effective Masses for Silicon Based Gate-All-Around Transistors," *Applied Sciences*, vol. 9, no. 9, p. 1895, 2019, DOI: 10.3390/app9091895.

[20] T. B. Boykin, G. Klimeck, and F. Oyafuso, "Valence band effective-mass expressions in the $sp^3d^5s^*$ empirical tight-binding model applied to a Si and Ge parametrization," *Physical Review B*, vol. 69, no. 11, pp. 115 201–1–10, 2004, DOI: 10.1103/PhysRevB.69.115201.

[21] "QuantumATK version O-2018.06," https://www.synopsys.com/silicon/quantumatk//, 2018, [Synopsys, inc., 2018].

[22] T. Sadi, C. Medina-Bailon, M. Nedjalkov, J. Lee, O. Badami, S. Berrada, H. Carrillo-Nuñez, V. Georgiev, S. Selberherr, and A. Asenov, "Simulation of the Impact of Ionized Impurity Scattering on the Total Mobility in Si Nanowire Transistors," *Materials*, vol. 12, no. 1, p. 124, 2019, DOI: 10.3390/ma12010124.

[23] "Garand User Guide [online]," https://solvnet.synopsys.com//, 2017, [Synopsys, inc., 2018].

[24] D. Esseni and F. Driussi, "A quantitative error analysis of the mobility extraction according to the Matthiessen rule in advanced MOS transistors," *IEEE Transactions on Electron Devices*, vol. 58, no. 8, pp. 2415–2422, 2011, DOI: 10.1109/TED.2011.2151863.

[25] N. Neophytou and H. Kosina, "Atomistic simulations of low-field mobility in si nanowires: Influence of confinement and orientation," *Physical Review B*, vol. 84, pp. 085 313 – 085 328, 2011, DOI: 10.1103/PhysRevB.84.085313.

[26] A. Cros, K. Romanjek, D. Fleury, S. Harrison, R. Cerutti, P. Coronel, B. Dumont, A. Pouydebasque, R. Wacquez, B. Duriez *et al.*, "Unexpected mobility degradation for very short devices: A new challenge for CMOS scaling," in *2006 International Electron Devices Meeting*. IEEE, 2006, pp. 1–4, DOI: 10.1016/10.1109/IEDM.2006.346872.

[27] R. Wang, H. Liu, R. Huang, J. Zhuge, L. Zhang, D.-W. Kim, X. Zhang, D. Park, and Y. Wang, "Experimental investigations on carrier transport in Si nanowire transistors: Ballistic efficiency and apparent mobility," *IEEE Transactions on Electron Devices*, vol. 55, no. 11, pp. 2960–2967, 2008, DOI: 10.1109/TED.2008.2005152.

[28] A. Svizhenko, M. Anantram, T. Govindan, B. Biegel, and R. Venugopal, "Two-dimensional quantum mechanical modeling of nanotransistors," *Journal of Applied Physics*, vol. 91, no. 4, pp. 2343–2354, 2002, DOI: 10.1063/1.1432117.

[29] S. Berrada, T. Dutta, H. Carrillo-Nunez, M. Duan, F. Adamu-Lema, J. Lee, V. Georgiev, C. Medina-Bailon, and A. Asenov, "NESS: new flexible Nano-Electronic Simulation Software," in *2018 International Conference on Simulation of Semiconductor Processes and Devices (SISPAD)*. IEEE, 2018, pp. 22–25, DOI: 10.1109/SISPAD.2018.8551701.